Magneto-optical properties of excitonic complexes in GaAs self-assembled quantum dots

M. Abbarchi,[1,2,*] T. Kuroda,[1] T. Mano,[1] K. Sakoda,[1] and M. Gurioli[2]
[1]*National Institute for Materials Science, 1-1 Namiki, Tsukuba 305-0044, Japan*
[2]*Dipartimento di Fisica, CNISM, Università di Firenze and European Laboratory for Non-Linear Spectroscopy, Via Sansone 1, Sesto Fiorentino 50019, Italy*

(Received 6 August 2009; revised manuscript received 12 October 2009; published 27 January 2010)

We report a detailed experimental investigation of the magneto-optical properties of different excitonic complexes (neutral exciton, neutral biexciton, and charged exciton) confined in self-assembled GaAs/AlGaAs strain-free quantum dots grown by droplet epitaxy, where all piezoelectric effects are lacking. We measured the Landè g factor and the diamagnetic coefficient γ for several quantum dots spanning an interval of $\sim$200 meV of the emission energy. The dependence of g and γ on quantum dot size and shape is discussed together with a comparison with Stranski-Krastanov and fluctuation-induced GaAs quantum dots, as well as with excitons confined in quantum wells.

DOI: 10.1103/PhysRevB.81.035334 PACS number(s): 78.55.Cr, 78.67.−n, 78.20.Ls, 73.21.La

I. INTRODUCTION

Spin properties of excitons confined in semiconductor quantum dots (QDs) have sparked off a great interest in the scientific community for a long time. The comprehension of the influence of the three-dimensional confinement on the Coulomb interaction among the constituent charge carriers, as well as of the excitonic response in a magnetic field, is needed to control and manipulate the charge and the spin of excitons in QD. This is expected to be of the utmost importance for the understanding of fundamental physics in solid state and for technological applications such as spin-based devices, quantum computation, and quantum information protocols.[1–4] On one side, the manipulation of the local Zeeman effect has been recently proposed[5,6] for the realization of single qubit logical operation. On the other side, the orientation of the fluctuating nuclear spins is one of the key to suppress the carriers spin dephasing in QDs, leading to the fascinating scenario of future quantum control scheme.

The excitonic complexes inside the QDs consist of multiplets coming up from different number of electrons (e) and holes (h) and their relative spin configurations.[7] Usually biexciton (XX) and trion (T) recombination are observed in the single QD emission spectra together with the neutral exciton line (X): XX and T lines are observed for the presence of other charges in addition to a single e-h pair. These levels may show a fine-structure splitting (FSS) determined by the exchange interaction that couples the spins of electrons and holes[8] and eventually by the interaction with a magnetic field. The exciton spin state splitting, at zero field, depends on the symmetry of the Hamiltonian which can result in characteristic degeneracy among these states.[7,8] The appearance of symmetry breaking is due to several intrinsic and extrinsic factors such as strain field in the crystal structure,[8] atomistic effect,[9] and geometric factors such as elongation[10] (for instance, the anisotropy of the specific crystal surface on which the QDs are grown can produce an asymmetric shape of the nanocrystal).

When a magnetic field is present, the exciton state splitting is also realized through the Zeeman interaction between carriers spin and the field. Moreover the exciton energy increases quadratically with the field through a diamagnetic coefficient γ which depends on the carrier confinement but also on the Coulomb interaction.[11] Finally, when the interaction with nuclear spins becomes strong, the Overhauser shift of the excitons energy has to be considered.[12,13]

Several studies have reported the magneto-optical properties of exciton in III-V QDs, involving spin-spin and spin-field interactions, much less is known on XX and T states to date. However, we note that the large part of the literature deals with InGaAs/GaAs, InAlAs/AlGaAs, InAs/InP, and InP/GaInP QDs (Refs. 1, 7, and 14–18) grown with conventional Stranski-Krastanov (SK) technique, which is based on self-aggregation driven by strain field associated to lattice mismatched materials. In all these nanostructures the electronic properties (transition energy, electron-hole overlap, fine-structure splitting, etc.) are strongly dependent not only on QD shape and size but also on the segregation, strain, and piezoelectric effects which vary from dot to dot and are not known with sufficient accuracy. In particular the e-h wavefunction separation related to piezoelectricity of strained material is expected to induce strong variation in the diamagnetic coefficient γ which reflects the overall extent of the exciton in the QD.[11,19] Furthermore the local displacement and the complicate interplay of the segregation, strain, and piezoelectric effects make the theoretical models poorly predictive.

Here we present a detailed investigation of the fine structure of the excitonic complexes (X, XX, and T) in strain-free GaAs QDs grown by droplet epitaxy (DE) studied by microphotoluminescence (μPL) experiments. In particular, by studying the excitonic level splitting without and with applied magnetic field, we extrapolate information about the QDs size and shape.

GaAs/AlGaAs heterostructures are known to be lattice matched systems (lattice mismatch $\simeq$0.06%). Thus all the strain and piezoelectric effects on the QDs electronic properties are absent in GaAs QDs. In contrast to the fluctuation-induced GaAs QDs (Ref. 13) [exciton localized in quantum wells (QWs)], our self-assembled QDs produce a high lateral confinement (see further details in the following Sec. IV), due to the high aspect ratio of the nanostructure together with a higher circular symmetry. Furthermore GaAs/AlGaAs

QDs allows a direct comparison with the well-studied two-dimensional QWs counterpart which is impossible in the conventional SK QDs. Moreover the DE-QDs emission energy precisely matches the high efficiency region of silicon-based detectors ($\simeq$70% in the range 650 ± 50 nm) with the additional advantage of enhancing radiative probability of the excitonic emission with respect to near IR emission typical in SK QDs. These features are very promising for many optoelectronic and spintronic devices which are useful for various applications such as linear-optics quantum computation[20] and free-space quantum cryptography.[21]

The paper is organized as follows: in Sec. II a description of the level structure of GaAs QDs is given together with a review of the spin-magnetic field interaction. In Sec. III the experimental details of the sample growth and QDs morphology are given together with a brief description of the experimental apparatus. In Sec. IV we describe the general features of the DE QDs electronic structure and photoluminescence in zero magnetic field. In Sec. V the polarization resolved magneto-PL measurements are shown and the fine structure of X, T, and XX is discussed together with the Landè g factor and the γ diamagnetic shift. Finally the conclusions are drawn in Sec. VI.

II. EXCITONIC LEVEL STRUCTURE

In this section the fine structure, the Zeeman interaction, and the diamagnetic shift of the energy levels related to X, T, and XX are analyzed. The scheme of X and XX spectra is reported in Fig. 1. Here we will take into account only the contribution of heavy-hole (h-h) band neglecting that of light-hole (l-h). Indicating the e and h spin in the z direction as S_z and J_z, respectively, the four h-h X states in the $|S_z;J_z\rangle$ basis are $\Psi_X=|\pm 1/2;\pm 3/2\rangle$. The separation of the related energy levels is due to the anisotropic exchange interaction and can be measured in absence of magnetic field (see Sec. IV).[8] The only optically active states are $\Psi_{X\downarrow}=|+1/2;-3/2\rangle$ and $\Psi_{X\uparrow}=|-1/2;+3/2\rangle$ and are called *bright excitons* while the other two are optically inactive and are said *dark excitons*.[7,22]

Let us now start with the discussion of the case of zero magnetic field. Assuming a perfect cylindrical symmetry along the z axis the bright exciton does not show any splitting.[8] This is represented in the bottom panel of Fig. 1 where XX and X spectra are shown. In In(Ga)As/GaAs QDs the cylindrical symmetry is usually broken by the effect of strain or atomistic effects resulting in a FSS from tens to hundreds of microelectron volts of the emitted photons energy[8,9] (see the central panel of Fig. 1) while in GaAs strain-free QDs the FSS, as reported in Refs. 10 and 23, is as a consequence of shape anisotropy or extrinsic effects.[24] The two resulting energy levels recombine emitting two photons with opposite linear polarization ($\parallel$ and $\perp$ in Fig. 1).

The biexciton state XX is formed when two excitons are confined in the QD. The configuration of the carriers spin in conduction band (CB) and valence band (VB) is determined by Pauli's principle and the total spin of XX is zero. Thus, the energy levels of XX are essentially free from the effect of anisotropic exchange interaction. However, in presence of a

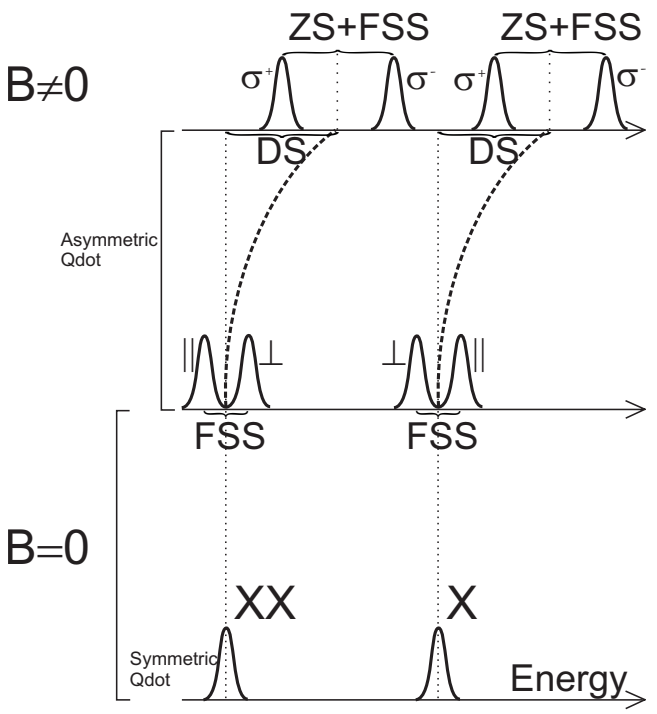

FIG. 1. PL spectra scheme of XX and X for a III-V QD without and with applied magnetic field. The bottom (central) panel refers to a symmetric (asymmetric) QD when $B=0$. The top panel displays the case of an asymmetric QD when $B \neq 0$. $\parallel$, $\perp$, and $\sigma^{\pm}$ indicate the linear and circular photon polarizations. Note that the proportion of the typical line shift and splitting are not respected in the pictures.

FSS in the X state the recombination path of the XX is twofold and the PL spectrum results in two split lines. The energy distance between the two photons emitted in the XX recombination is the same of the neutral exciton while the polarization of the two lines is mirror symmetric respect to the X doublet (central panel of Fig. 1). This feature is the fingerprint of the XX-X cascade.

In the case of T recombination the single carrier in CB (VB) in the initial state interacts with a zero spin in the filled VB (CB). Similar considerations hold for the final state of the T recombination. The exchange interaction vanishes and the T recombination is not split if $B=0$.[7]

By the application of a magnetic field in Faraday configuration ($B \parallel z$, where z is the growth direction), the energy levels are split into the Zeeman multiplets (this is the picture shown in the top panel of Fig. 1). All the three excitonic complexes X, XX, and T undergo similar magneto-optical phenomena, which can be mainly summarized in two effects, as reported by the equation

$$E_\alpha(B) = E_\alpha(0) \pm \mu_B g_\alpha B + \gamma_\alpha B^2, \tag{1}$$

where the index α=X,XX,T labels the specific excitonic complex, $\mu_B=5.79\times 10^{-5}$ eV/T is the Bohr magneton, g_α is the Landè factor, and γ_α is the diamagnetic constant.

The second term of the right side of Eq. (1) is the Zeeman interaction which results in the spin splitting of the levels, linear in the applied field. Experimentally it is possible to

extract the g_α factor for the different excitonic complexes by measuring the energy splitting of the corresponding circularly polarized lines and using the following relation:

$$g_\alpha = \frac{E_\alpha^{\sigma^+} - E_\alpha^{\sigma^-}}{\mu_B B} \tag{2}$$

[$\sigma^\pm$ labels the split line with clockwise (+) and anticlockwise (−) polarizations]. In Faraday geometry, the value of g_X is mainly determined by the height of the QDs, similarly to the case of QWs where it is ruled by the well width. The QDs (QWs) having smaller height (width) have a more negative value of g_X.[17,22] For relatively large height (width) of the QDs (QWs) the value of g_X can be positive and a change in sign is found when reducing the size.[17,22]

The third term in Eq. (1) is the diamagnetic shift γ_α, an increase in energy of both the two spin-split levels with magnetic field. This can be measured by a quadratic fit of $(E_\alpha^{\sigma^+}+E_\alpha^{\sigma^-})/2$. Exciton diamagnetic coefficients are of considerable interest because they are taken to be a measure of the effects of confinement and are used to estimate exciton binding energies.[11,19,25,26]

It is commonly believed that g_α simply reflects the carrier properties and for X, XX, and T can be considered the same. This hypothesis is confirmed by experimental evidences as recently reported for InAs QDs.[11] The exciton diamagnetic shift γ_X, depends on the QD spatial confinement to which excitons are subjected. When the limit of weak applied magnetic field is concerned [$a_0/l_B \ll 1$, where a_0 is the exciton Bohr radius and $l_B=\sqrt{\hbar/(eB)}$ is the magnetic length] is commonly accepted that the diamagnetic coefficient is a measure of the lateral size of the QDs. More precisely γ_X is proportional to the in-plane exciton wave-function mean-square expectation value $\langle x_X^2 \rangle$,

$$\gamma_X = \frac{e^2 \langle x_X^2 \rangle}{8\mu}, \tag{3}$$

where μ is the exciton reduced mass.[19] In conclusion, a complete characterization of the magneto-optical effects gives information on the exciton confinements in all the three spatial dimensions.

III. SAMPLE GROWTH AND EXPERIMENTAL DETAILS

The experiments were performed on GaAs self-assembled QDs in an $Al_{0.3}Ga_{0.7}As$ barrier, grown by DE in a conventional molecular-beam epitaxy apparatus.[27] The sample was then annealed at 680 °C for 1 h. In our case the DE growth allows the realization of samples with a wide spread of surface density and for single nanostructures study the very low value of 6–10 QD/μm^2 is also achievable. Besides, with this type of growth it is possible to control the spread of size distribution and thus to study different sized emitters on the same sample which gives the advantage of a similar surrounding environment. By far-field PL measurement, collecting the light from a huge number of QDs, we find an emission energy spanning over 250 meV.[28] The detailed description of the sample growth and its optical characterization are available in Refs. 27–29.

We used a confocal μPL setup. The light collected by the main collection microscopy objective (NA=0.42) was focused by a second microscopy objective in a single mode optical fiber with a core diameter of 3.5 μm so that we could reach the necessary lateral resolution of ~1 μm. The sample was cooled down to 4–10 K in a low-vibration, cold-finger cryostat with liquid He. The excitation beam was focused in a small spot (~1 μm of diameter) on the sample by using a beam splitter and the same collection objective. The CW excitation was performed above the barrier energy and was provided by a HeNe laser emitting at 534 nm preventing the Overhauser effect. The PL collected in the confocal optical fiber was fed into a grating monochromator.

The fine structure of excitons in absence of magnetic field was investigated by using a half-wave plate inserted in front of a linear polarizer between the two microscope objectives in order to discriminate the linear polarization of the PL. In this case we used a high spectral resolution setup (Jobin-Yvon double-grating monochromator, 1 m focal length) by which we could distinguish line broadening smaller than 15 μeV (in full width at half maximum, FWHM) and line shift as small as 5 μeV.

The magneto-optical investigation was performed by using a magnetic field in Faraday configuration ($\vec{B} \| z$, where z is the growth direction). The magnetic field was provided by a superconductive, He-cooled coil surrounding the cryostat and was finely tuned up to 5 T. The circularly polarized PL, resulting from the recombination of the split energy levels corresponding to different spin configuration, was analyzed with a quarter-wave plate and a linear polarizer between the two objectives. In the end the PL was dispersed and detected with the usual configuration of a 50 cm single grating spectrometer and a silicon-based charge-coupled-device camera reaching a spectral resolution of 200 μeV (FWHM).

IV. EXPERIMENTAL RESULTS

Typical high-resolution PL spectra of a single DE GaAs/AlGaAs QD without applied magnetic field is shown in Fig. 2(a) in the two main linear polarization channels (θ=0 and θ=90 which correspond to $[1\bar{1}0]$ and [110]). We used here an intermediate excitation power density that is slightly below the exciton saturation level. Note also that no signature of line splitting can be found with unpolarized PL detection.[30] The polarization resolved PL allows for a precise attribution of the different excitonic complexes and to estimate the FSS of the excitons energy levels in zero magnetic field. Moreover with this analysis we can also determine the asymmetry axes of the QD confining potential. In Fig. 2(b) the XX and X PL lines (left and right panels) corresponding to the orthogonal polarizations θ=0 and θ=90 are fitted with two Gaussian profiles corresponding to the split doublet. Reporting the intensity of each component in a polar graph [see Fig. 2(c), left and right panels refer to XX and X cases, respectively] we can determine the polarization axes. As a matter of fact the observation of the mirror-symmetric polarization splitting of the two lines X and XX is a direct way to assess the nature of the recombination lines in single QDs emission spectra. The measured FSS for X and XX in Fig. 2

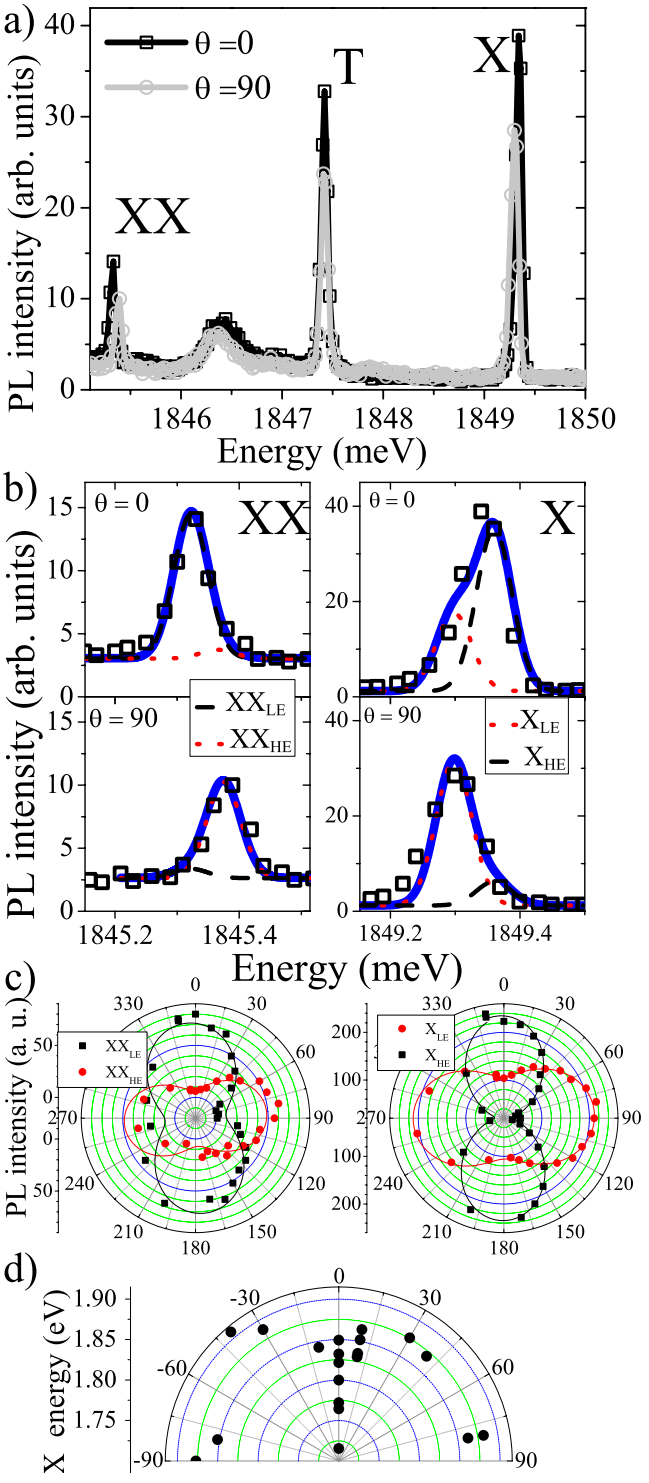

FIG. 2. (Color online) (a) Linearly polarized PL spectra of a GaAs DE QD (obtained with the high-resolution setup). The three main lines correspond to X, T, and XX. (b) (Left) Right panels show the decomposition of (XX) X line in the two split components $(XX_{HE})X_{HE}$ and $(XX_{LE})X_{LE}$ for the spectra shown in (a) (squares). Dashed and dotted curves are Gaussian fit of the split components and continuous line is the sum of the two. (c) Symbols: polar plot of the polarization intensity of $(XX_{HE})X_{HE}$ and $(XX_{LE})X_{LE}$ lines [(left) right panel]; the solid lines are sinusoidal fit to data. (d) Polar plot of X emission energy as a function of polarization axis for different QDs.

are −48 and 43 μeV, respectively. The T line does not show any FSS, within the experimental error, when rotating the polarization detection. This allows us to attribute this line to the charged exciton complex T. These attributions of the X, XX, and T lines are confirmed on the basis of intensity-correlation investigation[31,32] measured with an Hanbury-Brown and Twiss interferometer and power dependence analysis[33] (not shown here). Finally, in GaAs QDs, the unintentional residual doping turns out to be *p* type and the dominant T term is attributed to positively charged trions. The XX and T binding energy, measured as the energy distance from the corresponding X line is always positive and usually are in the intervals 3–4 and 0.7–2 meV, respectively.

The polarization resolved measurements shown in Fig. 2(b) provides information on the polarization axes of the QD PL. This analysis for all the polarization directions allows us to trace the polarization intensity of all the XX and X components as shown in the two polar plot of Fig. 2(c). The same investigation on several nanoemitters shows that, when increasing the QD emission energy, (i) the FSS starts decreasing and (ii) the polarization axes of DE QDs are oriented along different directions and not only along the $[1\bar{1}0]$.[10] These two effects start to be evident for QD emitting at energy higher than 1.82 meV and becomes more relevant at very high energy. The reduction in the FSS can be attributed to two different origins. From morphological analysis we found that a reduction in size also increases the QD symmetry and this obviously produces a reduction in FSS.[10] In addition, the value of 1.82 meV also corresponds to the onset of electron delocalization out of the QDs due to the wave-function penetration into the barrier region (see later the discussion of the diamagnetic shift). Assuming that for small QDs the hole wave function is still well localized due to its heavier mass, we expect that the FSS will decrease with the decreasing QD size. This occurs because the electron wave function is now less sensitive to the dot shape anisotropy and the electron-hole wave-function overlap is reduced.[11,34]

The second point, that is the random orientation of the polarization axis, highlights the role of extrinsic effects as significant contribution in determining the QD potential anisotropy.[24] We relate these extrinsic effects to the presence of charged traps in the QD environment.[30] The Coulomb interaction between confined charges and external-charged traps, acting as an additional electric field, determines a preferential direction for the polarization axes along the line connecting the QDs and the charged trap.[10,24] This picture closely follows the well-established spectral diffusion model that explains the inhomogeneous broadening of the single QDs exciton lines, which, in our case, is on the order of 100 μeV.[30] Recently a different picture, based on atomic scale randomness, was used to explain the random orientation of the FSS in alloy of InGaAs QDs.[9] We believe that this theory does not apply to our GaAs QDs. We also exclude relevant variations in the QDs composition associated to materials interdiffusion possibly due to postgrowth annealing.[35]

The present findings agree with the simple picture shown in the central panel of Fig. 1 and allow a clear attribution of all the three main excitonic complexes giving direct information on the QD shape and environment.

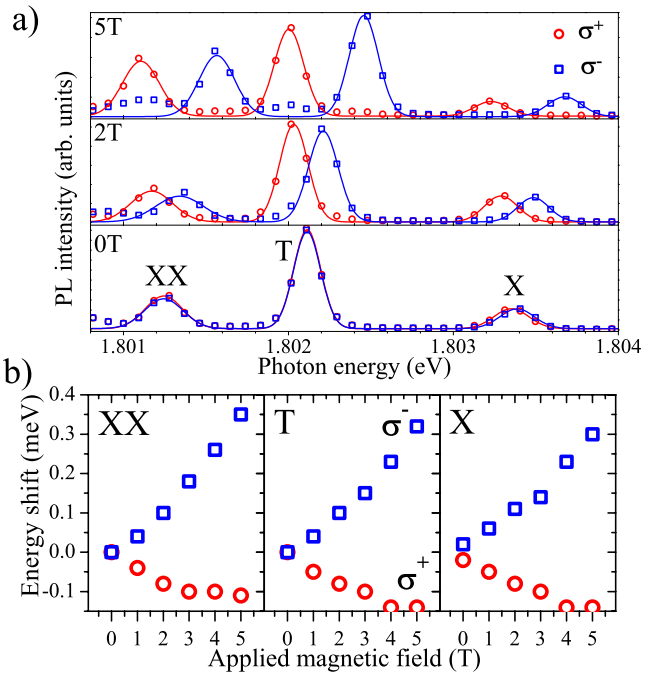

FIG. 3. (Color online) (a) PL spectra of a single QD at different magnetic field for the two circular photon polarizations $\sigma^{\pm}$. The solid lines are Gaussian fit to data. (b) Peak position of the XX, T, and X doublets as a function of the magnetic field.

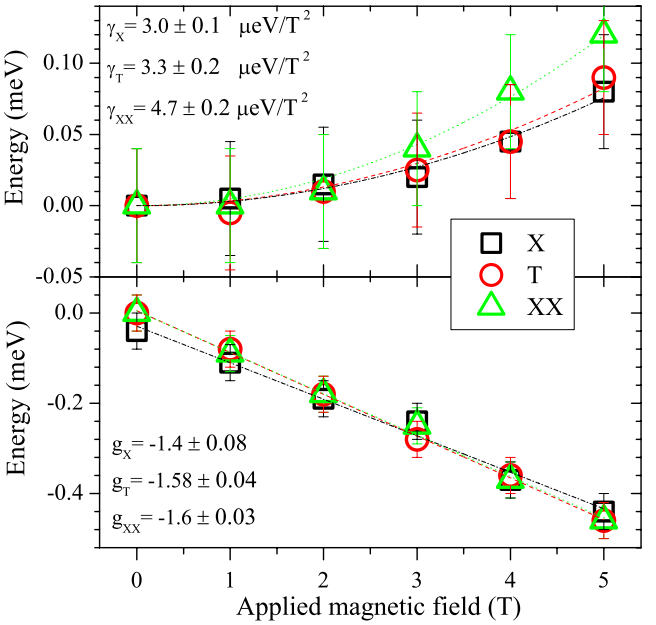

FIG. 4. (Color online) Upper panel: average energy shift of the two split α lines (α=X,T,XX) for determining the diamagnetic shift. The dashed lines are parabolic fit to data. Lower panel: splitting of the two α lines for determining the Landè g_α factor. The dashed lines are linear fit to data.

V. MAGNETOPHOTOLUMINESCENCE

Circularly polarized PL spectra of a GaAs QD under applied magnetic field are shown in Fig. 3(a). With this low-resolution experimental setup and due to the relatively small FSS observed in the DE QDs,[10] in the case B=0, the two opposite circularly polarized contributions to the QD PL are identical within the experimental error. Increasing the applied magnetic field, each emission line splits into an oppositely circularly polarized doublet. The peak positions for XX, T, and X recombination lines, as obtained by a Gaussian fit of the PL spectra, are reported in Fig. 3(b).

The diamagnetic shift for the three lines is reported in the upper panel of Fig. 4 while the energy difference of the two split contributions, which represents the Zeeman shift and it is linear in B, is reported in the lower panel of Fig. 4. The present phenomenology is consistent with the discussion presented in Sec. II and schematically described in the top panel of Fig. 1. On the basis of the relationship of Eq. (1) previously defined, we can measure g_α and γ_α by fitting the experimental data (as shown by the dashed lines in Fig. 4).

The spread of emission energy of the GaAs QDs allows us to study the size dependence of g_α and γ_α coefficients. All the measured g_X factors are summarized in Fig. 5, where our findings are compared with the data obtained by Snelling *et al.*[22] in QWs and by Gammon *et al.*[13] for fluctuation-induced QDs in 4.2-nm-thick GaAs/AlGaAs QW. For all the investigated DE QDs g_X is always negative, tends to decrease with the QD emission energy, and varies between −0.8 and −1.9. Important information is obtained by the comparison of our data with other GaAs unstrained nanostructures. The QW data show a large variation in g_X from 0.3 to −1.8 when reducing the well thickness from 15 to 3 nm. Moreover, the two thinnest QWs, respectively, of 6 and 3 nm width[22] show a reduction in g_X more than a factor 2, from −0.8 to −1.8. More important is that all the g_X data of DE QDs are included in this interval. Referring now to fluctuation-induced QDs in 4.2-nm-thick GaAs/AlGaAs QW,[13] the value of g_X =−1.3 is almost in the middle of the values found for the 3 and 6 nm QWs. From the analysis of all these data we conclude that g_X is mainly determined by the dimension of the exciton confinement parallel to the magnetic field and it is almost independent on the lateral confinement, in agreement with recent findings.[17] We suggest that the height of DE QDs are quite small (possibly few nanometers) and varies only

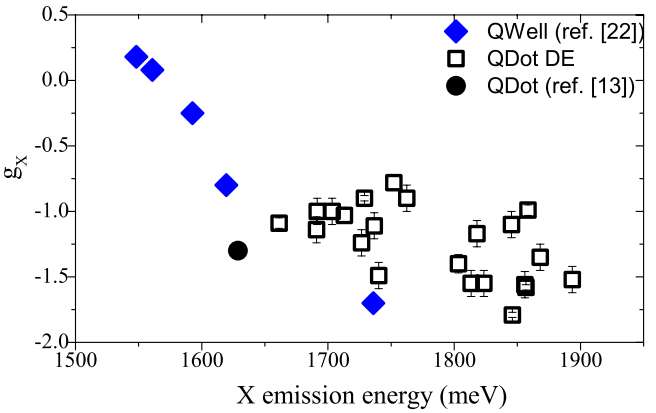

FIG. 5. (Color online) Landè g_X factor for QW (Ref. 22) (full diamonds), our self-assembled QDs (open squares) and native QDs (Ref. 13) (full circle) reported as a function of the X emission energy.

slightly when increasing the emission energy. This variation in the QD height is not sufficient to explain the 200 meV variation in the QD emission energy and important changes in the lateral confinement are expected.

It is also interesting comparing our results with recent findings on InAs/InP (Ref. 17) and In(Ga)As/GaAs QDs (Ref. 36) where the size dependence of g_X has been studied. Accordingly with our results a decrease in g_X is found when increasing the QD emission energy.[17,36] However the sign of g_X is changed (as in the case of GaAs QWs) and the values are, for InAs/InP QDs, in the range from +0.8 to −2.0 (Ref. 17) for an almost equivalent change in the emission energy (200 meV) as compared to our data. The authors conclude that for InAs/InP QDs (differently to the case of DE QDs) the emission energy is mainly determined by the height of the QDs. Even smaller values, down to $g_X=-3$ have been reported for InAs/GaAs.[11,36] The analogies between strained InAs and strain-free GaAs QDs and QWs points out the relevance of the geometrical factors in reducing the g_X when reducing the QD height: reducing the QD height will result in more negative values of g_X.[17] Positive values of g_X are only found in quite large InAs/InP QDs and GaAs QWs, denoting that the lack of strong confinement brings the change in the sign of g_X. In our case, we conclude that all the investigated QDs are in the limit of strong vertical confinement and at the same time the observed data also bring us to suggest a minor role of the strain and piezoelectric effects in controlling the g_X factor.

The comparison between the Landè factors for the different excitonic complexes points out that g_{XX} and g_T result very similar to g_X, as already reported in the literature.[11] However the data are largely scattered and only a statistical analysis can bring useful information. Besides the strong data fluctuations, we find that the average values of the statistical distributions are: $g_X=-1.25\pm0.29$, $g_T=-1.30\pm0.33$, and $g_{XX}=-1.60\pm0.36$ (the error is expressed as standard deviation).

Let us now discuss the diamagnetic shift. The values of γ_α are found to be quite similar (even if not identical) for the different excitonic complexes: $\gamma_X\simeq\gamma_T\simeq\gamma_{XX}$. Therefore we concentrate our analysis on the value of γ_X, hereafter simply labeled as γ. Following the commonly accepted model, we expect that the coefficient γ will be a measure of the exciton lateral confinement by Eq. (3). From the typical values of the reduced mass (in GaAs $\mu=0.06m_o$, with m_o is the electron mass) we conclude that the typical values of $\gamma=6$ $\mu eV/T^2$ gives an exciton radius on the order of 4 nm, denoting that also the strong lateral confinement condition is fulfilled. A further confirmation of this conclusion arises from the comparison with fluctuation-induced GaAs/AlGaAs QDs,[13] where a value of $\gamma=25$ $\mu eV/T^2$ is given, showing a much smaller exciton lateral confinement with respect to our DE GaAs QDs. Much larger values are also found in QWs up to ~100 $\mu eV/T^2$ (Ref. 37); in this case the lateral confinement of carriers is defined by the exciton Bohr radius and the diamagnetic shift has been also used to determine the exciton binding energy.[37] Finally, for SK QDs, the values of γ reported in literature usually spread from 3 $\mu eV/T^2$ (Ref. 19) to 10 $\mu eV/T^2$,[15,36] not so far from our finding. Again we conclude that only a minor role is played by strain-induced effect in controlling the value of γ.

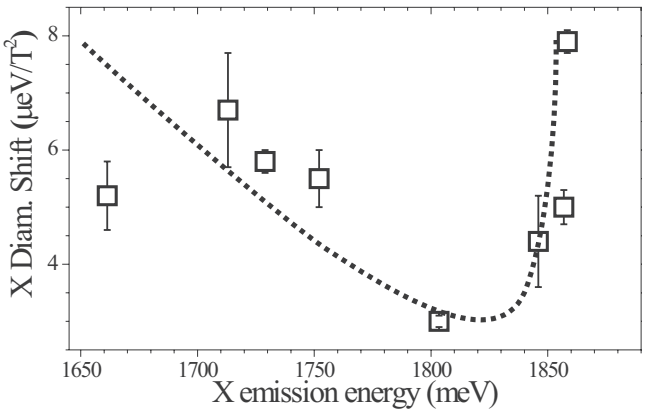

FIG. 6. X diamagnetic shift as a function of the X emission energy. The dashed line is a guide to the eyes.

At the same time Eq. (3) can be used to extract the trend of the lateral confinement when varying the QD size. We have already pointed out that we expect a significant variation in the lateral confinement in the DE QDs, differently to the case of InAs/InP QDs.[17] Assuming that the lateral confinement is reflected in the emission energy (as suggested by the analysis of g_X), we report in Fig. 6 the summary of the measured γ as a function of the X emission energy. The expected trend consists in a smooth reduction in γ down to a minimum followed by a sharp increase in γ due to the electron penetration into the barrier as soon as the confinement energy become comparable with the barrier potential height.[19] This prediction is in agreement with our results, as shown by the eye-guide dashed line in the graph which qualitatively reproduces the theoretical trend.[19]

Finally we note that the increase in γ starts at ~1.82 eV which, as already pointed out in the end of Sec. IV, corresponds to the energy at which the FSS starts to decrease[10] and the polarization axes becomes randomly oriented (see eye-guide). To our understanding this is mainly due to a combination of two different effects, both arising when the QD size decreases. The smaller is the QDs the higher is its circular symmetry and the larger is the wave-function penetration into the barrier. Both effects are responsible for the reduction in the FSS but they are not simply related to the randomization of the polarization axes. However, we can also speculate that there could be a correlation between the penetration of the excitonic wave function in the barrier material and the extrinsic contribution to the FSS arising from random charges trapped nearby the QDs.[10,24]

VI. CONCLUSIONS

We have studied the magneto-optical properties of different excitonic complexes in DE GaAs QDs by means of μPL measurements. We have accurately attributed the single QD emission lines to different excitonic complexes, such as neutral and charged excitons and biexcitons, determining the FSS at zero field. From the PL spectra in presence of a magnetic field both the Landè and the diamagnetic factor are obtained. Their values are compared with the previous find-

ings and expected trends as a function of the QD size. We conclude that the DE QDs are in the limit of strong vertical and lateral confinement and at the same time we suggest a minor role of the strain and piezoelectric effects in controlling the QDs magneto-optical properties.

ACKNOWLEDGMENTS

This work was partially supported by the Italian PRIN MIUR under Contract No. 2006022932. T.K. and T.M. acknowledge partial support of a Grant-in-Aid from MEXT, Japan.

*Author to whom correspondence should be addressed. abbarchi.marco@nims.go.jp

[1] D. Bouwmeester, A. Ekert, and A. Zeilinger, *The Physics of Quantum Information* (Springer, Berlin, 2000).
[2] O. Benson, C. Santori, M. Pelton, and Y. Yamamoto, Phys. Rev. Lett. **84**, 2513 (2000).
[3] R. M. Stevenson, R. J. Young, P. Atkinson, K. Cooper, D. A. Ritchie, and A. J. Shields, Nature (London) **439**, 179 (2006).
[4] N. Akopian, N. H. Lindner, E. Poem, Y. Berlatzky, J. Avron, D. Gershoni, B. D. Gerardot, and P. M. Petroff, Phys. Rev. Lett. **96**, 130501 (2006).
[5] B. E. Kane, Nature (London) **393**, 133 (1998).
[6] R. Vrijen, E. Yablonovitch, K. Wang, H. W. Jiang, A. Balandin, V. Roychowdhury, T. Mor, and D. DiVincenzo, Phys. Rev. A **62**, 012306 (2000).
[7] M. Bayer, G. Ortner, O. Stern, A. Kuther, A. A. Gorbunov, A. Forchel, P. Hawrylak, S. Fafard, K. Hinzer, T. L. Reinecke, S. N. Walck, J. P. Reithmaier, F. Klopf, and F. Schafer, Phys. Rev. B **65**, 195315 (2002).
[8] R. Seguin, A. Schliwa, S. Rodt, K. Pötschke, U. W. Pohl, and D. Bimberg, Phys. Rev. Lett. **95**, 257402 (2005).
[9] V. Mlinar and A. Zunger, Phys. Rev. B **79**, 115416 (2009).
[10] M. Abbarchi, C. A. Mastrandrea, T. Kuroda, T. Mano, K. Sakoda, N. Koguchi, S. Sanguinetti, A. Vinattieri, and M. Gurioli, Phys. Rev. B **78**, 125321 (2008).
[11] M.-F. Tsai, H. Lin, C.-H. Lin, S.-D. Lin, S.-Y. Wang, M.-C. Lo, S.-J. Cheng, M.-C. Lee, and W.-H. Chang, Phys. Rev. Lett. **101**, 267402 (2008).
[12] T. Belhadj, T. Kuroda, C.-M. Simon, T. Amand, T. Mano, K. Sakoda, N. Koguchi, X. Marie, and B. Urbaszek, Phys. Rev. B **78**, 205325 (2008).
[13] D. Gammon, Al. L. Efros, T. A. Kennedy, M. Rosen, D. S. Katzer, D. Park, S. W. Brown, V. L. Korenev, and I. A. Merkulov, Phys. Rev. Lett. **86**, 5176 (2001).
[14] M. Bayer, T. Gutbrod, A. Forchel, V. D. Kulakovskii, A. Gorbunov, M. Michel, R. Steffen, and K. H. Wang, Phys. Rev. B **58**, 4740 (1998).
[15] N. I. Cade, H. Gotoh, H. Kamada, H. Nakano, and H. Okamoto, Phys. Rev. B **73**, 115322 (2006).
[16] G. A. Narvaez, G. Bester, and A. Zunger, Phys. Rev. B **72**, 245318 (2005).
[17] N. A. J. M. Kleemans, J. van Bree, M. Bozkurt, P. J. van Veldhoven, P. A. Nouwens, R. Notzel, A. Yu. Silov, P. M. Koenraad, and M. E. Flatte, Phys. Rev. B **79**, 045311 (2009).
[18] D. Kim, W. Sheng, P. J. Poole, D. Dalacu, J. Lefebvre, J. Lapointe, M. E. Reimer, G. C. Aers, and R. L. Williams, Phys. Rev. B **79**, 045310 (2009).
[19] K. L. Janssens, F. M. Peeters, and V. A. Schweigert, Phys. Rev. B **63**, 205311 (2001).
[20] E. Knill, R. Laflamme, and G. J. Milburn, Nature (London) **409**, 46 (2001).
[21] C. H. Bennett, G. Brassard, and A. K. Eckert, Sci. Am. **267**(4), 50 (1992).
[22] M. J. Snelling, E. Blackwood, C. J. McDonagh, R. T. Harley, and C. T. B. Foxon, Phys. Rev. B **45**, 3922 (1992).
[23] D. Gammon, E. S. Snow, B. V. Shanabrook, D. S. Katzer, and D. Park, Phys. Rev. Lett. **76**, 3005 (1996).
[24] R. Ferreira, Physica E (Amsterdam) **13**, 216 (2002).
[25] A. Wojs and P. Hawrylak, Solid State Commun. **100**, 487 (1996).
[26] S. Raymond, P. Hawrylak, C. Gould, S. Fafard, A. Sachrajda, M. Potemski, A. Wojs, S. Charbonneau, D. Leonard, P. M. Petroff, and J. L. Merz, Solid State Commun. **101**, 883 (1997).
[27] N. Koguchi, S. Takahashi, and T. Chikyow, J. Cryst. Growth **111**, 688 (1991).
[28] V. Mantovani, S. Sanguinetti, M. Guzzi, E. Grilli, M. Gurioli, K. Watanabe, and K. Koguchi, J. Appl. Phys. **96**, 4416 (2004).
[29] K. Watanabe, N. Koguchi, and Y. Gotoh, Jpn. J. Appl. Phys., Part 2 **39**, L79 (2000).
[30] M. Abbarchi, F. Troiani, C. Mastrandrea, G. Goldoni, T. Kuroda, T. Mano, K. Sakoda, N. Koguchi, S. Sanguinetti, A. Vinattieri, and M. Gurioli, Appl. Phys. Lett. **93**, 162101 (2008).
[31] T. Kuroda, T. Belhadj, M. Abbarchi, C. Mastrandrea, M. Gurioli, T. Mano, N. Ikeda, Y. Sugimoto, K. Asakawa, N. Koguchi, K. Sakoda, B. Urbaszek, T. Amand, and X. Marie, Phys. Rev. B **79**, 035330 (2009).
[32] T. Kuroda, M. Abbarchi, T. Mano, K. Watanabe, M. Yamagiwa, K. Kuroda, K. Sakoda, G. Kido, N. Koguchi, C. Mastrandrea, L. Cavigli, M. Gurioliand, Y. Ogawa, and F. Minami, Appl. Phys. Express. **1**, 042001 (2008).
[33] M. Abbarchi, C. Mastrandrea, T. Kuroda, T. Mano, A. Vinattieri, K. Sakoda, and M. Gurioli, J. Appl. Phys. **106**, 053504 (2009).
[34] R. J. Young, R. M. Stevenson, A. J. Shields, P. Atkinson, K. Cooper, D. A. Ritchie, K. M. Groom, A. I. Tartakovskii, and M. S. Skolnick, Phys. Rev. B **72**, 113305 (2005).
[35] T. Mano, T. Kuroda, K. Mitsuishi, M. Yamagiwa, X.-J. Guo, K. Furuya, K. Sakoda, and N. Koguchi, J. Cryst. Growth **301-302**, 740 (2007).
[36] T. Nakaoka, T. Saito, J. Tatebayashi, and Y. Arakawa, Phys. Rev. B **70**, 235337 (2004).
[37] S.-L. Tyan, P. A. Shields, R. J. Nicholas, F.-Y. Tsai, and C.-P. Lee, Jpn. J. Appl. Phys., Part 1 **39**, 3286 (2000).